E-Band Characterization of 3D-Printed Dielectrics for Fully-Printed Millimeter-Wave Wireless System Packaging

Bijan K. Tehrani*, Ryan A. Bahr*, Wenjing Su*, Benjamin S. Cook†, and Manos M. Tentzeris*
*School of Electrical and Computer Engineering, Georgia Institute of Technology, Atlanta, GA, USA
†Kilby Labs, Texas Instruments, Dallas, TX, USA

***Abstract*—This work explores the integration of 3D and inkjet printing manufacturing processes with millimeter-wave (mm-wave) wireless packaging technology. Stereolithography-based (SLA) 3D printing methods are discussed for two classes of materials: polymeric and ceramic-loaded dielectrics. 3D-printed materials are characterized for performance within the E-band wireless regime (55–95 GHz), extracting relative permittivity and loss tangent. Thermal cycling tests are performed in order to evaluate the thermal stress characteristics of the printed dielectrics structures. Die encapsulation with SLA printing technology is presented as an alternative to the standard molding and stamping technology. Inkjet printing is used to demonstrate the fabrication of metallic structures directly onto 3D-printed packages, highlighting potential applications of on-package antenna arrays, lenses, and metamaterial surfaces. Finally, inkjet-printed mm-wave transmission lines are realized on 3D-printed ramp structures, demonstrating efficient 3D interconnects with ramp slopes up to 65° for through-mold-via (TMV) solutions.**

***Index Terms*—Mm-wave characterization, mm-wave packaging, interconnects, SoP, inkjet printing, 3D printing.**

I. Introduction

Current trends in emerging wireless technologies are pushing for the realization of high-bandwidth data transmission and miniaturized form factor, along with a simultaneous reduction in cost. This next generation of mobile communication systems, such as 5G and vehicle-to-vehicle (V2V), has taken root in the field of millimeter-wave (mm-wave) wireless technology, where carrier frequencies operate within the range of tens to hundreds of gigahertz. In order to miniaturize wireless systems and reduce detrimental high-frequency parasitics, the realization of system-on-package (SoP) packaging solutions is an area of popular research, where integrated circuit (IC) dies can be directly integrated with peripheral components, such as other ICs, antennas, and various other passive components.

A practical means to realize these SoP solutions is through the use of additive manufacturing. Currently, additive manufacturing methods are gaining an increasing interest as an alternative to traditional methods for the reduction of material waste and production cost [1]. Additionally, inkjet and 3D printing allow for the selective deposition of materials in a 3D fashion, where dielectric and metallic patterns can be fabricated directly onto virtually any host to create fully-printed, vertically-integrated electronic systems and packages [2], [3]. Specifically from a wireless perspective, inkjet printing offers the advantage of incorporating printed antenna structures and interconnects with wireless dies and packages in an efficient SoP scenario [4], [5]. The continued study of the materials and processes behind these additive printing techniques allows for the integration and innovation of advanced fabrication methods to realize emerging wireless system designs within the mm-wave regime [6]–[8].

This paper outlines the processing and electronic characterization of two 3D-printed stereolithography-based (SLA) dielectric materials in the mm-wave regime. Polymeric and ceramic-loaded resins are printed and characterized for the first time at E-band (55–95 GHz), where relative permittivity and loss tangent are extracted. Plus, samples of these printed dielectrics undergo thermal cycling in order to assess thermal stress characteristics. Potential applications of these 3D-printed SLA materials are presented, including printed die encapsulation as well as use as an RF substrate for on-package antenna arrays and periodic metamaterial structures. Finally, inkjet-printed mm-wave transmission lines are integrated with 3D-printed ramp structures with slopes up to 65° to demonstrate the feasibility of on-package integration through additive printing manufacturing methods.

II. Materials and Processes

SLA printing utilizes the selective photonic exposure and crosslinking of a photopolymer solution to create a solid 3D object, where resolution is determined by the minimum increment of the build plate stepper motor and the resolution of the digital light processing (DLP) or laser source. The materials used with SLA printing consist of photopolymer resins that crosslink through exposure to ultraviolet (UV) and near-UV radiation (300–400 nm). Vorex (orange color) from MadeSolid and Porcelite from Tethon3D are photoresins designed to cure at UV wavelengths between 350–410 nm. Vorex is an acrylate-based resin focused on impact strength and toughness. Porcelite is a crystalline silica-loaded resin with the ability to fire at 1000 °C into a fully porcelain object, however the inclusion of ceramic composites in the resins have to potential to allow for an increase in permittivity to enable use as a dielectric for applications where firing is not desired.

The proof-of-concept 3D structures are printed using a custom LittleRP SLA 3D printer with a Viewsonic PJD7820HD, a 1080p DLP projector focused at a distance to provide 38 μm X/Y resolution based on the pixel size with 3000 lm intensity over a 41.5×72 mm stainless steel build plate. For this effort, a glass slide is affixed to the steel build plate using a photopolymer adhesive to act as a removable printing host and facilitate sample handling. Printed layer thickness is determined by the Z-axis stepper motor and is chosen to be 50 μm for a balance of resolution and processing speed. The

978-1-5090-6360-4/17/$31.00 ©2017 IEEE

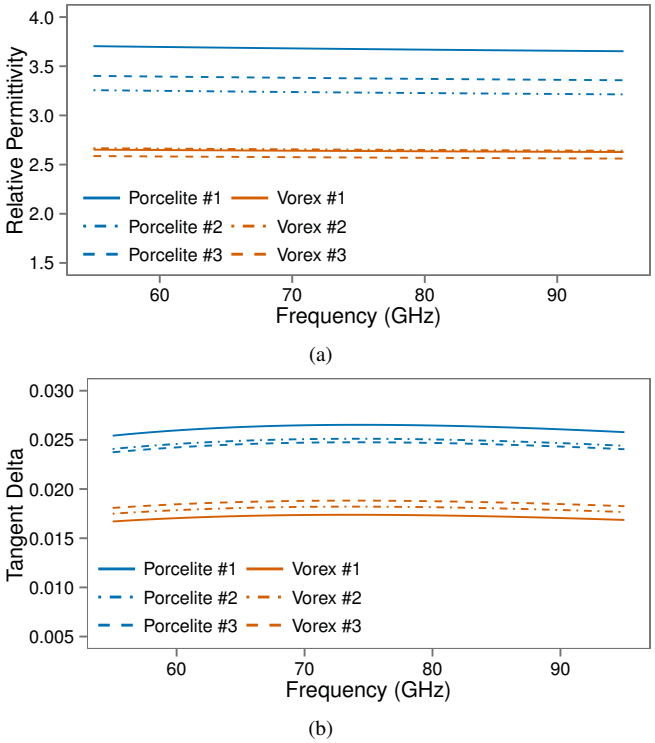

Fig. 1. E-band characterization of (a) relative permittivity and (b) loss tangent for 3D-printed SLA materials extracted from S-parameters.

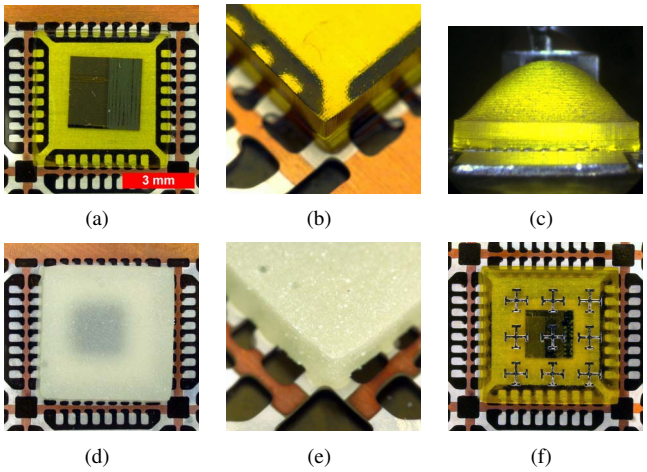

Fig. 2. 3D-printed die encapsulations on a metallic QFN leadframe: Vorex encapsulation (a) top view and (b) perspective view, (c) Vorex dielectric lens structure; Porcelite encapsulation (d) top view and (e) perspective view; (f) Vorex encapsulation with inkjet-printed metamaterial.

50 µm layers are exposed for 7 sec to cure Vorex and 15 sec to cure Porcelite. After all layers are exposed and printed, the samples are submerged in two isopropyl alcohol (IPA) baths in order to remove the majority of the residual unexposed material and then any remainder from the first bath. Finally, a post-print 1 J/cm^2 UV exposure is performed to fully cure the 3D-printed Vorex and Porcelite samples.

As a preliminary mechanical evaluation, 5×5×1 mm samples of Vorex and Porcelite are fabricated and exposed to 25 thermal cycles with the following profile: -40 °C to 125 °C with a ramp of approximately 2 °C/min. From a visual inspection, the thermal cycling does not have any effect on the samples, where no cracking or deformation is observed.

III. Dielectric Characterization

The accurate dielectric characterization of these 3D-printed SLA materials is necessary in order to efficiently simulate and fabricate mm-wave wireless systems in an additive and robust fashion. Waveguide fills with dimensions 3.01×1.55×1 mm are fabricated in order to fill 1 mm thick WR-12 waveguide spacer shims. An Agilent N5242A PNA-X is used along with VDI WR12-VNAX frequency extenders to enable E-band measurements of the SLA dielectric samples.

Modeling methods satisfying the Kramers–Kronig relation are used to extract the relative permittivity and loss tangent of the printed materials from the measured S-parameters. Fig. 1. shows the extracted measurements of (a) relative permittivity and (b) loss tangent for the printed samples over the range of 55–95 GHz. Relative permittivity (ϵ_r) measurements appear stable and fairly linear for frequencies up to above 90 GHz with a small downward slope as frequency increases. As expected, the ceramic-loaded Porcelite material exhibits a higher ϵ_r due to the presence of high-ϵ_r ceramic composites. The variation of the ϵ_r measurements for the Porcelite material are likely the result of dimensional variations for the waveguide fill samples due to the developing tuning of the processing conditions for this resin. Currently, relative permittivity measurement variations of less than ±2% and ±7% are achieved for the Vorex and Porcelite samples, respectively. Loss tangent (tan δ) measurements yield maximums of 0.019 and 0.026 for the Vorex and Porcelite samples, respectively, demonstrating their suitability for mm-wave RF applications.

IV. 3D-Printed Die Encapsulation

The printing of an IC die encapsulation using the above SLA materials is presented with the goal of replacing standard epoxy molding and stamping methods of package encapsulation. In addition to being an ambient-pressure room-temperature fabrication process, SLA printing allows for the simple realization of selectively-patterned and nontraditionally-shaped encapsulation solutions, while simultaneously maintaining tan δ within the same range of standard epoxy molding compound materials [9].

Silicon dies with 280 µm thickness and areas of 2×2 mm and 3×3 mm are attached to a metallic QFN leadframe using an inkjet-printed polymer-based ink. After the dies are attached, 5.5×5.5×1 mm encapsulations are printed directly onto the dies using the Vorex and Porcelite materials and the outlined processing conditions. This is accomplished by affixing the QFN leadframes to the build plate of the SLA printer in order to directly pattern the die encapsulations onto the leadframes. Fig. 2 presents images of the printed Vorex and Procelite encapsulations. In addition to the standard encapsulation, an SLA printing tool can be configured to fabricate

978-1-5090-6360-4/17/$31.00 ©2017 IEEE

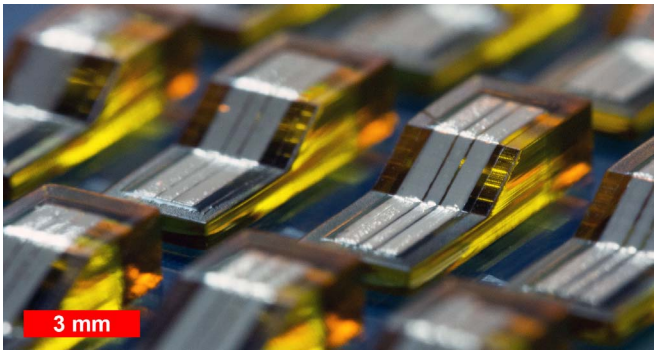

(a)

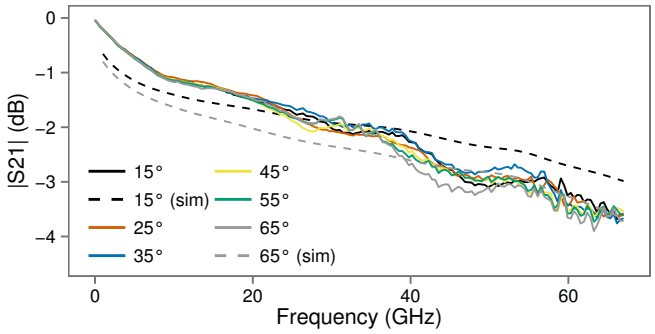

(b)

Fig. 3. (a) 3D-printed ramp structures with inkjet-printed CPW interconnects, highlighting the 35° slope ramps. (b) |S21| insertion loss measurements (—) and simulations (– –) of printed CPW TMVs with varying slope.

nontraditional encapsulation shapes, for example open cavities for microelectromechanical systems (MEMS) sensors and dielectric lenses for package-integrated antennas, presented in Fig. 2(c). These novel package shapes can be achieved by simply changing the 3D model in the SLA printing tool, highlighting the reconfigurable nature of this technology for diverse application-specific packaging applications.

This newly demonstrated SLA printing technology for packaging can be easily combined with existing inkjet printing technology to realize the post-process fabrication of on-package components, including passive components, antennas, sensors, and metamaterial structures. Fig. 2(f) presents a periodic frequency selective surface (FSS) inkjet-printed directly onto a 3D-printed encapsulation using a Dimatix DMP-2831 inkjet printing system and silver nanoparticle-based ink for such applications as wireless filtering and aperture coupling.

V. Sloped mm-Wave Interconnects for Printed SoP

With the ability to inkjet print electronic structures directly onto a 3D-printed encapsulation, interest is placed onto how these structures can interface with a molded IC within the package. The concept of directly interconnecting a molded IC die to an external plane of its encapsulation is an area not widely covered in literature. Amkor Technology Inc. (Chandler, AZ, USA) has demonstrated a through-mold-via (TMV) process for package-on-package (PoP) integration, however interconnects are limited to solder balls typically used with ball grid array (BGA) packages [10]. Due to the interest in SoP design solutions for mm-wave wireless systems, efficient TMV interconnects in the mm-wave regime are desired to expand the possibilities of system integration.

The integration of inkjet printing with 3D printing technology requires an analysis of the capabilities of this typically 2/2.5D technology in truly 3D applications. In order to evaluate SLA 3D printing technology for integration with inkjet printing for mm-wave packaging, ramped interconnect structures with slopes ranging from 15–75° are characterized with the Vorex SLA material. Sample Vorex ramps measuring 3×7.5 mm with a 1 mm tall ramp and 10 µm layer height resolution are fabricated with the LittleRP SLA printer to represent the sloped walls of an IC encapsulation. Next, two layers of a MicroChem SU-8 polymer-based ink are printed onto the ramp structure in order to passivate the 10 µm layer steps of the 3D-printed ramps with a film thickness of approximately 8–12 µm. Sun Chemical EMD5730 silver nanoparticle-based ink is printed to pattern coplanar waveguide (CPW) interconnect lines from the die-level to the encapsulation-level of the ramp structures. Finally, the printed ramp interconnects are sintered in an oven at 150 °C for 1 hr to complete the fabrication process. Fig. 3(a) shows a perspective micrograph of the test vehicle containing multiple samples of the SLA ramps with varying slope. |S21| insertion loss of the printed TMV interconnects is characterized up to 67 GHz with an Agilent E8361C PNA and 67A-GSG-250-C probes from GGB, presented in Fig. 3(b) along with simulations for the two extreme cases (15° and 65°). All slopes ranging from 15–65° exhibit an insertion loss between 0.5–0.6 dB/mm at 60 GHz, where the 75° slope did not achieve complete electrical connectivity. The printed 3D interconnects presented in this paper yield a 10x reduction in insertion loss from standard wirebond interconnects at 60 GHz [11].

VI. Conclusion

This work outlines the processing and electronic characterization of two 3D-printed SLA dielectric materials: Vorex (orange) and Porcelite. These polymeric and ceramic-loaded resins are printed and characterized at E-band (55–95 GHz) where relative permittivity and loss tangent are extracted. Relative permittivity measurements are within the expected range for polymer-based dielectrics, where an expected increase in permittivity is present with the ceramic-loaded material. Samples of these printed dielectrics undergo thermal cycling in order to assess thermal stress characteristics, yielding no visible cracks or physical deformation. Potential applications of these 3D-printed SLA materials are also presented, including printed die encapsulation as well as use as an RF substrate for on-package antenna arrays, lenses, and periodic metamaterial structures. Finally, inkjet-printed CPW transmission lines are combined with 3D-printed ramp structures with slopes ranging from 15–65° for use as mm-wave TMV interconnects. The integration of 3D and inkjet printing technologies has the potential to enable the realization of fully-printed on-demand arbitrarily-shaped SoP wireless packages for such emerging

978-1-5090-6360-4/17/$31.00 ©2017 IEEE

applications as automotive radar and 5G mobile communication.

ACKNOWLEDGMENT

The authors would like to acknowledge SRC (Task 2663.001) and Texas Instruments for their support with this work.

REFERENCES

[1] J. G. Hester, S. Kim, J. Bito, T. Le, J. Kimionis, D. Revier, C. Saintsing, W. Su, B. Tehrani, A. Traille *et al.*, "Additively manufactured nanotechnology and origami-enabled flexible microwave electronics," *Proceedings of the IEEE*, vol. 103, no. 4, pp. 583–606, 2015.

[2] A. J. Lopes, E. MacDonald, and R. B. Wicker, "Integrating stereolithography and direct print technologies for 3d structural electronics fabrication," *Rapid Prototyping Journal*, vol. 18, no. 2, pp. 129–143, 2012.

[3] T. Merkle, R. Gotzentzen, J. Y. Choi, and S. Koch, "Polymer multichip module process using 3-d printing technologies for d-band applications," *IEEE Transactions on Microwave Theory and Techniques*, vol. 63, no. 2, pp. 481–493, Feb 2015.

[4] B. Tehrani, B. Cook, and M. Tentzeris, "Post-process fabrication of multilayer mm-wave on-package antennas with inkjet printing," in *Antennas and Propagation Society International Symposium (APS/URSI), 2015 IEEE*, July 2015.

[5] ——, "Inkjet-printed 3d interconnects for millimeter-wave system-on-package solutions," in *Microwave Symposium (IMS), 2016 IEEE MTT-S International*, June 2016.

[6] P. I. Deffenbaugh, R. C. Rumpf, and K. H. Church, "Broadband microwave frequency characterization of 3-d printed materials," *IEEE Trans. Compon. Packag. Manuf. Technol.*, vol. 3, no. 12, pp. 2147–2155, Dec 2013.

[7] Y. Arbaoui, V. Laur, A. Maalouf, and P. Queffelec, "3d printing for microwave: Materials characterization and application in the field of absorbers," in *IEEE International Microwave Symposium (IMS 2015)*, 2015.

[8] A. L. Vera-Lopez, E. A. Rojas-Nastrucci, M. Cordoba-Erazo, T. Weller, and J. Papapolymerou, "Ka-band characterization and rf design of acrynolitrile butadiene styrene (abs)," in *2015 IEEE MTT-S International Microwave Symposium*, May 2015, pp. 1–4.

[9] L. Li, A. Kapur, and K. B. Heames, "Characterization of transfer molding effects on rf performance of power amplifier module," in *2004 IEEE 54th Electronic Compon. and Technol. Conference (ECTC)*, vol. 2, 2004, pp. 1671–1677.

[10] A. Yoshida, S. Wen, W. Lin, J. Kim, and K. Ishibashi, "A study on an ultra thin pop using through mold via technology," in *2011 IEEE 61st Electronic Compon. and Technol. Conference (ECTC)*, May 2011, pp. 1547–1551.

[11] T. Krems, W. Haydl, H. Massler, and J. Rudiger, "Millimeter-wave performance of chip interconnections using wire bonding and flip chip," *1996 IEEE MTT-S International Microwave Symposium Digest*, 1996.

978-1-5090-6360-4/17/$31.00 ©2017 IEEE